Electronic Research Archive

https://www.aimspress.com/journal/era

ERA, 34(5): 3481–3502.
DOI: 10.3934/era.2026155
Received: 15 February 2026
Revised: 08 April 2026
Accepted: 13 April 2026
Published: 22 April 2026

Research article

Dynamics of a state feedback impulsive predator-prey model incorporating fear effect and additional food supply

Meng Zhang* **and Jiayi Zheng**

School of Science, Beijing University of Civil Engineering and Architecture, Beijing 100044, China

* **Correspondence:** Email: zhangmengbucea@126.com.

Abstract: This study proposes a predator-prey model that incorporates fear effects and additional food provision. A theoretical analysis is conducted by first establishing the positivity and boundedness of solutions, and then examining the existence and stability of all feasible equilibria. Models with unilateral and bilateral impulsive state feedback control are further introduced and analyzed. For these controlled systems, sufficient conditions for the existence and orbital asymptotic stability of order-1 periodic solutions are derived. Numerical simulations are provided to support the theoretical findings, showing excellent agreement with the analytical results. Finally, a systematic sensitivity analysis is performed to quantify the influence of the prey's fear factor and the total amount of additional food on the system dynamics.

Keywords: fear; additional food; predator-prey model; successor function; order-1 periodic solution

1. Introduction

Predation is a fundamental interactive mechanism that governs the dynamic balance of populations in ecosystems. Classical predator-prey models have primarily focused on the direct effects of predation through consumptive interactions—i.e., the reduction of prey populations due to feeding. However, extensive empirical studies over recent decades have shown that prey species can perceive predator presence, leading to non-consumptive "fear effects" that profoundly alter demographic traits and behaviors [1–3]. Such fear-induced responses can trigger adaptive changes in prey behavior, activity patterns, and reproductive strategies—even in the absence of direct mortality—resulting in suppressed population growth rates [4]. For example, Zanette et al. [5] demonstrated in song sparrows that exposure to predator cues caused a 40% decline in offspring production, highlighting the ecological significance of perceived predation risk. Complementing empirical findings, Sasmal [6] developed a single-species model showing how fear can substantially reduce the per capita growth rate of prey, providing a theoretical basis for incorporating psychological fear into ecological models.

In parallel, the intentional provision of additional food has become a widely adopted ecological management strategy aimed at enhancing predator populations or restoring ecosystem stability. In agricultural and conservation settings, supplying alternative food sources can divert predation pressure, reduce interference among predators, and improve the biological control of pest species [7–9]. For instance, in rice paddies, supplementary feeding of natural enemies has been shown to increase predator efficiency and abundance, thereby reducing crop damage [10]. The ecological ramifications of additional food are multifaceted: While it may lower the direct predation rate on focal prey by offering alternative resources, it can also enhance predator fitness, recruitment, and interaction rates, potentially leading to unintended outcomes such as prey extinction or destabilization of population dynamics. Mathematical ecologists have extensively studied the role of additional food in predator-prey systems, noting that variations in the quality and quantity of such resources can critically influence system behavior—from promoting coexistence to triggering extinction. In particular, Srinivasu et al. [11] emphasized the importance of handling times for different food types in shaping community structure, while Ghorai and Poria [12] demonstrated that additional food can induce complex spatiotemporal dynamics in ecological models.

Both fear effects and additional food represent significant factors in ecological theory and practice, each contributing to the nuanced regulation of predator-prey interactions. However, their combined influence remains underexplored within a unified theoretical framework. A notable contribution by Mondal et al. [7] introduced a predator-prey model that integrates both mechanisms:

$$\begin{cases} \dfrac{dx}{dt} = \dfrac{rx}{1+ky} - d_1 x - a_1 x^2 - \dfrac{a_2 xy}{b_1 + \alpha\mu A + x}, \\ \dfrac{dy}{dt} = \dfrac{ca_2(x+\mu A)y}{b_1 + \alpha\mu A + x} - d_2 y, \end{cases} \tag{1.1}$$

where x ($ind \cdot m^2$) and y ($ind \cdot m^2$) denote prey and predator densities respectively; r (d^{-1}) and a_2 ($ind^{-1} \cdot m^2 \cdot d^{-1}$) are intrinsic growth rates of prey and predator; d_1 (d^{-1}) and d_2 (d^{-1}) represent natural mortality rates; a_1 ($ind^{-1} \cdot m^2 \cdot d^{-1}$) is the intraspecific competition coefficient of prey; b_1 ($ind \cdot m^{-2}$) is the half-saturation constant; c (dimensionless) is the efficiency with which predators convert food into growth; k (dimensionless) quantifies the fear effect; μA ($ind \cdot m^{-2}$) reflects the effective quantity of additional food; and α signifies its nutritional quality.

Building on this foundation, the present study develops a dynamic predator-prey model that incorporates both fear effects and the provision of additional food. The remainder of this paper is structured follows. In Section 2, we rigorously analyze the positivity and boundness of solutions, along with the existence and stability of equilibria. In Sections 3 and 4, we extend the model to include unilateral and bilateral impulsive state-feedback controls, and systematically investigate the existence and orbital asymptotic stability of order-1 periodic solutions under such control strategies. Section 5 presents numerical simulations that validate the theoretical results and illustrate the ecological implications of fear and additional food in shaping population dynamics. Finally, in Section 6, the vole-weasel predation model from the chapter on grassland ecosystems is introduced to illustrate how theoretical research can inform real-world ecological case studies. Through this integrated analytical and numerical approach, we aim to deepen the understanding of how behavioral and resource mediated mechanisms interact to influence the long-term stability and complexity of ecological systems.

2. Model

Considering the fear factor and the provision of additional food to the predator in model (1.1), we developed a predator-prey model:

$$\begin{cases} \dfrac{dx}{dt} = \dfrac{rx}{1+ky} - d_1 x - a_1 x^2 - \dfrac{a_2 xy}{b+A+x}, \\ \dfrac{dy}{dt} = \dfrac{ca_2(x+\theta A)y}{b+A+x} - d_2 y, \end{cases} \tag{2.1}$$

where b ($ind \cdot m^{-2}$) is the half-saturation factor; A ($ind \cdot m^{-2}$) is the total amount of additional food released to predators; θ (dimensionless) is the efficiency with which predators recognize, capture, and utilize additional food; and k (dimensionless) represents the prey's fear factor of the predator.

To facilitate the subsequent analysis, we recall some prerequisite concepts. A generalized planar impulsive semi-dynamical system with state-dependent feedback control can be described as follows [13, 14]:

$$\begin{cases} \left.\begin{aligned} \frac{dx}{dt} &= P(x,y), \\ \frac{dy}{dt} &= Q(x,y), \end{aligned}\right\} if \phi(x,y) \neq 0, \\ \left.\begin{aligned} \Delta x &= A(x,y), \\ \Delta y &= B(x,y). \end{aligned}\right\} if \phi(x,y) = 0. \end{cases}$$

Lemma 2.1. *(Analogue of Poincaré criterion [14,15]) The order-n periodic solution $\pi(t) = (\xi(t), \eta(t))$ of the system is orbitally asymptotically stable if $|\mu| < 1$, where*

$$\mu = \prod_{j=1}^{n} \Delta_j \exp\left[\int_0^T \left(\frac{\partial P}{\partial \xi} + \frac{\partial Q}{\partial \eta}\right)_{(\xi(t),\eta(t))} \mathrm{d}t\right],$$

with

$$\Delta_j = \frac{P_+\left(\frac{\partial B}{\partial \eta}\frac{\partial \phi}{\partial \xi} - \frac{\partial B}{\partial \xi}\frac{\partial \phi}{\partial \eta} + \frac{\partial \phi}{\partial \xi}\right) + Q_+\left(\frac{\partial A}{\partial \xi}\frac{\partial \phi}{\partial \eta} - \frac{\partial A}{\partial \eta}\frac{\partial \phi}{\partial \xi} + \frac{\partial \phi}{\partial \eta}\right)}{P\left(\frac{\partial \phi}{\partial \xi}\right) + Q\left(\frac{\partial \phi}{\partial \eta}\right)}.$$

$P_+ = P(\xi(t^+), \eta(t^+)), Q_+ = Q(\xi(t^+), \eta(t^+))$ and P, Q, $\frac{\partial A}{\partial \xi}$, $\frac{\partial A}{\partial \eta}$, $\frac{\partial B}{\partial \xi}$, $\frac{\partial B}{\partial \eta}$, $\frac{\partial \phi}{\partial \xi}$, $\frac{\partial \phi}{\partial \eta}$ are calculated at $(\xi(t), \eta(t))$.

2.1. Positivity and boundedness of solutions

Theorem 2.1. *All solutions of system* (2.1) *remain positive for all $t > 0$.*

Proof. Based on biological conditions, the initial conditions $x(0) > 0$, $y(0) > 0$. Then,

$$x(t) = x(0)\exp\left\{\int_0^t \left[\frac{r}{1+ky(s)} - d_1 - a_1 x(s) - \frac{a_2 y(s)}{b+A+x(s)}\right]\mathrm{d}s\right\} > 0,$$

$$y(t) = y(0)\exp\left\{\int_0^t \left[\frac{ca_2(x(s)+\theta A)}{b+A+x(s)} - d_2\right]\mathrm{d}s\right\} > 0.$$

Hence, the solutions of system (2.1) remain positive.

Theorem 2.2. *All solutions of system* (2.1) *are uniformly bounded.*

Proof. Let us consider the function $\omega(x, y) = x + \frac{1}{c}y$; then,

$$\begin{aligned}\frac{d\omega}{dt} &= \frac{rx}{1+ky} - d_1x - a_1x^2 + \frac{a_2\theta Ay}{b+A+x} - \frac{d_2y}{c}\\ &\leq \frac{rx}{1+ky} - d_1x + \frac{a_2\theta Ay}{b} - \frac{d_2y}{c}.\end{aligned}$$

When $\epsilon \leq min\left\{d_1, d_2 - \frac{ca_2\theta A}{b}\right\}$,

$$-d_1x + \frac{a_2\theta Ay}{b} - \frac{d_2y}{c} \leq -\epsilon\left(x + \frac{y}{c}\right) = -\epsilon\omega.$$

Then,

$$\frac{d\omega}{dt} \leq \frac{rx}{1+ky} - \epsilon\omega. \tag{2.2}$$

Based on system (2.1), we get

$$\lim_{t\to\infty} \sup x(t) \leq \frac{r-d_1}{a_1}.$$

Thus, (2.2) can be written as

$$\frac{d\omega}{dt} + \epsilon\omega \leq \frac{rx}{1+ky} \leq rx \leq r\left(\frac{r-d_1}{a_1}\right).$$

By using the comparison theorem [16], we get

$$0 \leq \omega(x, y) \leq \frac{r}{\epsilon}\left(\frac{r-d_1}{a_1}\right).$$

Hence, ω is bounded, $x > 0$ and $y > 0$, so, x and y are bounded.

2.2. Existence of equilibria and stability analysis

Theorem 2.3. *(i) System* (2.1) *always has two boundary equilibria $E_0(0,0)$ and $E_1(\frac{r-d_1}{a_1}, 0)$, where $r > d_1$.*
(ii) System (2.1) *has one positive equilibrium if $x^* > 0$, $A_2^2 - 4A_1A_3 > 0$, $A_3 < 0$; system* (2.1) *has no positive equilibrium if $x^* > 0$, $A_2^2 - 4A_1A_3 > 0$, $A_2 > 0$, $A_3 > 0$ or $A_2^2 - 4A_1A_3 = 0$, $A_2 > 0$, where $x^* = \frac{d_2(b+A)-ca_2\theta A}{ca_2-d_2}$, $A_1 = a_2k$, $A_2 = a_2 + (a_1kx^* + d_1k)(b + A + x^*)$, $A_3 = (d_1 + a_1x^* - r)(b + A + x^*)$ and $y^* = \frac{-A_2 \pm \sqrt{A_2^2-4A_1A_3}}{2A_1}$.*

Proof. If $y \neq 0$, let $\frac{dy}{dt} = 0$ and we get

$$x^* = \frac{d_2(b+A) - ca_2\theta A}{ca_2 - d_2}.$$

Then, substituting this into $\frac{\mathrm{d}x}{\mathrm{d}t} = 0$, we get

$$A_1 y^2 + A_2 y + A_3 = 0, \tag{2.3}$$

where

$$\begin{aligned} A_1 &= a_2 k > 0, \\ A_2 &= a_2 + (a_1 k x^* + d_1 k)(b + A + x^*) > 0, \\ A_3 &= (d_1 + a_1 x^* - r)(b + A + x^*). \end{aligned}$$

Then,

$$y^* = \frac{-A_2 \pm \sqrt{A_2^2 - 4A_1 A_3}}{2A_1}.$$

If $A_2^2 - 4A_1A_3 > 0$ and $A_3 < 0$, (2.3) has one positive root; if $A_2^2 - 4A_1A_3 > 0$, $A_2 > 0$ and $A_3 > 0$ or $A_2^2 - 4A_1A_3 = 0$ and $A_2 > 0$, (2.3) has no positive root.

Theorem 2.4. *(i) $E_0(0,0)$ is a saddle if $\frac{ca_2\theta A}{b+A} < d_2$; $E_0(0,0)$ is an unstable node or focus if $\frac{ca_2\theta A}{b+A} > d_2$.*
(ii) $E_1(\frac{r-d_1}{a_1}, 0)$ is LAS (locally asymptotically stable) if $\frac{ca_2(r-d_1)+ca_1a_2\theta A}{a_1b+a_1A+r-d_1} < d_2$; $E_1(\frac{r-d_1}{a_1}, 0)$ is a saddle if $\frac{ca_2(r-d_1)+ca_1a_2\theta A}{a_1b+a_1A+r-d_1} > d_2$.
(iii) The positive equilibrium E^* is LAS if $a_1(b + A + x^*)^2 > a_2y^*$; E^* is an unstable node or focus if $a_1(b + A + x^*)^2 < a_2y^*$.

Proof. The Jacobian matrix of system (2.1) around the equilibrium point E_0 is given by

$$J(E_0) = \begin{pmatrix} r - d_1 & 0 \\ 0 & \frac{ca_2\theta A}{b+A} - d_2 \end{pmatrix}.$$

Obviously, $r - d_1 > 0$, and $E_0(0,0)$ is unstable. Also, $E_0(0,0)$ is a saddle if $\frac{ca_2\theta A}{b+A} < d_2$; $E_0(0,0)$ is an unstable node or focus if $\frac{ca_2\theta A}{b+A} > d_2$.
The Jacobian matrix of system (2.1) around the equilibrium point E_1 is given by

$$J(E_1) = \begin{pmatrix} -r + d_1 & -\frac{rk(r-d_1)}{a_1} - \frac{a_2(r-d_1)}{a_1b+a_1A+r-d_1} \\ 0 & \frac{ca_2(r-d_1)+ca_1a_2\theta A}{a_1b+a_1A+r-d_1} - d_2 \end{pmatrix}.$$

Obviously, $-r + d_1 < 0$, so, if $\frac{ca_2(r-d_1)+ca_1a_2\theta A}{a_1b+a_1A+r-d_1} < d_2$, E_1 is LAS. If $\frac{ca_2(r-d_1)+ca_1a_2\theta A}{a_1b+a_1A+r-d_1} > d_2$, E_1 is a saddle.
The Jacobian matrix of system (2.1) around the equilibrium point E^* is given by

$$J(E^*) = \begin{pmatrix} -a_1x^* + \frac{a_2x^*y^*}{(b+A+x^*)^2} & -\frac{rkx^*}{(1+ky^*)^2} - \frac{a_2x^*}{b+A+x^*} \\ \frac{ca_2y^*(b+A-\theta A)}{(b+A+x^*)^2} & 0 \end{pmatrix}.$$

The characteristic equation is

$$\lambda^2 - \lambda\left[-a_1x^* + \frac{a_2x^*y^*}{(b + A + x^*)^2}\right] + \left[\frac{rkx^*}{(1 + ky^*)^2} + \frac{a_2x^*}{b + A + x^*}\right]\left[\frac{ca_2y^*(b + A - \theta A)}{(b + A + x^*)^2}\right] = 0.$$

By Viète's theorem,

$$\lambda_1 + \lambda_2 = -a_1x^* + \frac{a_2x^*y^*}{(b + A + x^*)^2}, \tag{2.4}$$

$$\lambda_1\lambda_2 = \left[\frac{rkx^*}{(1+ky^*)^2} + \frac{a_2x^*}{b+A+x^*}\right]\left[\frac{ca_2y^*(b+A-\theta A)}{(b+A+x^*)^2}\right]. \tag{2.5}$$

If $a_1(b+A+x^*)^2 > a_2y^*$ and $b+A > \theta A$, then $\lambda_1+\lambda_2 < 0$, $\lambda_1\lambda_2 > 0$, so $\lambda_1 < 0$, $\lambda_2 < 0$, and E^* is LAS.

If $a_1(b+A+x^*)^2 < a_2y^*$ and $b+A > \theta A$, then $\lambda_1+\lambda_2 > 0$, $\lambda_1\lambda_2 > 0$, so $\lambda_1 > 0$, $\lambda_2 > 0$, and E^* is an unstable node or focus.

If $b+A < \theta A$, then $\lambda_1\lambda_2 < 0$, λ_1 and λ_2 are positive and negative, respectively, and E^* is a saddle. However, $0 < \theta < 1$ and $\theta A < A$, so $b+A > \theta A$. The condition is not valid.

Theorem 2.5. *If the equilibrium point E^* is locally asymptotically stable, then E^* is globally asymptotically stable.*

Proof. Let

$$\nu(x,y) = \frac{1}{xy}, \gamma_1 = \frac{rx}{1+ky} - d_1x - a_1x^2 - \frac{a_2xy}{b+A+x}, \gamma_2 = \frac{ca_2(x+\theta A)y}{b+A+x} - d_2y.$$

Then,

$$\begin{aligned}\Delta(x,y) =& \frac{\partial}{\partial x}(\gamma_1\nu) + \frac{\partial}{\partial y}(\gamma_2\nu)\\ =& \frac{\partial}{\partial x}\left(\frac{r}{1+ky} - d_1 - a_1x - \frac{a_2y}{b+A+x}\right)\frac{1}{y} + \frac{\partial}{\partial y}\left[\frac{ca_2(x+\theta A)}{b+A+x} - d_2\right]\frac{1}{x}\\ =& -\frac{a_1}{y} + \frac{a_2}{(b+A+x)^2}.\end{aligned}$$

So, $\Delta(x,y) < 0$ if $a_2y < a_1(b+A+x)^2$. According to the Bendixson-Dulac theorem [6,7,17], there is no closed orbit around E^*. Hence, E^* is globally asymptotically stable.

3. Unilateral state-feedback impulse controls

When $a_1(b+A+x^*)^2 > a_2y^*$, E^* is a stable node or focus. In this case, we consider impulse control to maintain ecological balance. The following discussion is based on the assumption that there is only one positive equilibrium point, i.e., $A_2^2 - 4A_1A_3 > 0$ and $A_3 < 0$.

First, we calculate vertical isobars; let $\frac{dx}{dt} = 0$ and we get $x = 0$ and $\frac{a_2ky^2}{b+A+x} + \left(\frac{a_2}{b+A+x} + d_1k + a_1kx\right)y - r + d_1 + a_1x = 0$.

Then, we calculate horizontal isobars. Let $\frac{dy}{dt} = 0$ and we get $y = 0$ and $x = \frac{d_2(b+A)-ca_2\theta A}{ca_2-d_2}$.

3.1. Upper-threshold impulsive model

In concrete terms, when the number of y increases to a certain threshold h_1 and the number of x is less than $\frac{3}{2}x^*$, on the one hand, measures are taken (e.g., introduction of natural enemies, etc.) to reduce the number of y, and on the other hand, a certain amount of x is released. So, we get unilateral

state-feedback impulse control system:

$$\begin{cases} \left.\begin{aligned} \frac{dx}{dt} &= \frac{rx}{1+ky} - d_1 x - a_1 x^2 - \frac{a_2 xy}{b+A+x}, \\ \frac{dy}{dt} &= \frac{ca_2(x+\theta A)y}{b+A+x} - d_2 y, \end{aligned}\right\} x > \frac{3}{2}x^*,\ y \neq h_1, \\ \left.\begin{aligned} \Delta x &= \alpha, \\ \Delta y &= -\beta y, \end{aligned}\right\} 0 < x < \frac{3}{2}x^*,\ y = h_1. \end{cases} \tag{3.1}$$

The impulse set is

$$M_1 = \left\{ (x, y) \mid 0 < x < \frac{3}{2}x^*, y = h_1 \right\}.$$

The phase set is

$$N_1 = \{ (x, y) \mid x > 0, y = (1-\beta)\, h_1 \}.$$

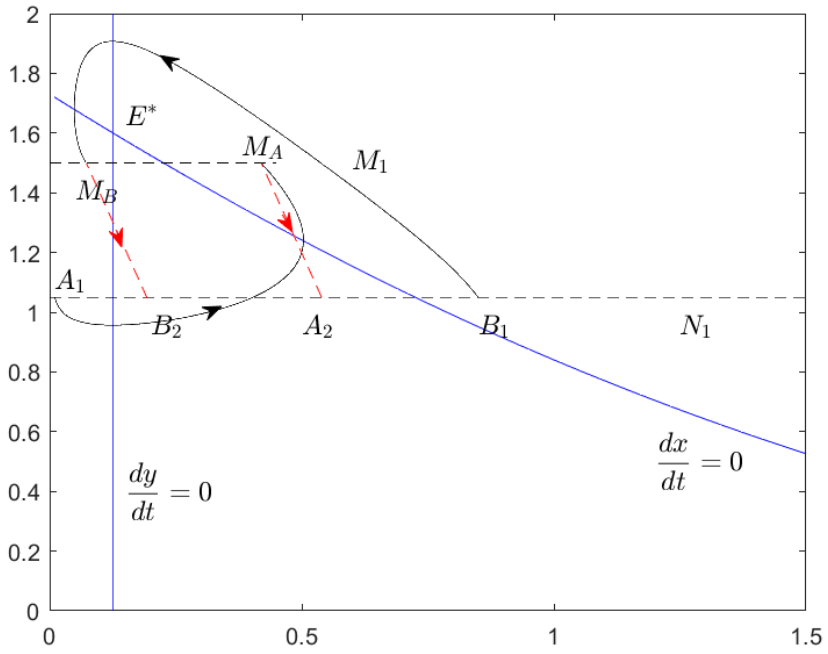

Figure 1. Unilateral order-1 periodic solutions.

Theorem 3.1. *System* (3.1) *possesses unilateral order-1 periodic solutions.*

Proof. As shown in Figure 1, we take a point M_A on M_1 such that $x_{M_A} > x_{E^*}$. Based on the trajectory direction of the system and the nature of the isobars, we can find a point A_1 on N_1 such that the trajectory from A_1 intersects M_1 at M_A and $x_{A_1} < x_{E^*}$. M_A maps to A_2 under impulsive action. So $x_{A_2} = x_{M_A} + \alpha > x_{E^*} > x_{A_1}$. Then, we get

$$F(A_1) = x_{A_2} - x_{A_1} > 0.$$

At the same time, we take a point B_1 on N_1 such that $x_{B_1} > x_{A_2}$, the trajectory from B_1 intersects M_1 at M_B, and $x_{M_B} < x_{E^*} < x_{M_A}$. And M_B maps to B_2 under impulsive action. So $x_{B_2} = x_{M_B} + \alpha$. Obviously, $x_{B_2} < x_{A_2} < x_{B_1}$. Then, we get

$$F(B_1) = x_{B_2} - x_{B_1} < 0.$$

By the continuity of the successor function [18], $\exists P \in (A_1, B_1)$ such that $F(P) = 0$. So system (3.1) possesses unilateral order-1 periodic solutions.

Theorem 3.2. *The unilateral order-1 periodic solution of system* (3.1) *is orbitally asymptotically stable if* $H(\xi_1 + \alpha, \xi_1) < H(\xi_1, \xi_1 + \alpha)$*, where*

$$H(x, y) = \frac{ca_2(x + \theta A)h_1 y}{b + A + x} - d_2 h_1 y.$$

Proof. Let $x = \xi(t)$, $y = \eta(t)$ be the unilateral order-1 periodic solution, and the period be T. As can be seen from system (3.1),

$$P(x, y) = \frac{rx}{1 + ky} - d_1 x - a_1 x^2 - \frac{a_2 xy}{b + A + x},$$

$$Q(x, y) = \frac{ca_2(x + \theta A)y}{b + A + x} - d_2 y,$$

$$A(x, y) = \alpha, B(x, y) = -\beta y, \phi(x, y) = y - h_1;$$

$$(\xi(0), \eta(0)) = (\xi_0, \eta_0),$$

$$(\xi(T), \eta(T)) = (\xi_1, \eta_1) = (\xi_1, h_1),$$

$$(\xi(T^+), \eta(T^+)) = (\xi_0, \eta_0) = (\xi_1 + \alpha, (1 - \beta)h_1).$$

We get

$$\frac{\partial P}{\partial x} = \frac{r}{1 + ky} - d_1 - 2a_1 x - \frac{a_2 y(b + A)}{(b + A + x)^2},$$

$$\frac{\partial Q}{\partial y} = \frac{ca_2(x + \theta A)}{b + A + x} - d_2,$$

$$\frac{\partial A}{\partial x} = 0, \frac{\partial A}{\partial y} = 0, \frac{\partial B}{\partial x} = 0, \frac{\partial B}{\partial y} = -\beta, \frac{\partial \phi}{\partial x} = 0, \frac{\partial \phi}{\partial y} = 1.$$

Then,

$$\begin{aligned}\Delta_1 &= \frac{P_+\left(\frac{\partial B}{\partial y}\frac{\partial \phi}{\partial x} - \frac{\partial B}{\partial x}\frac{\partial \phi}{\partial y} + \frac{\partial \phi}{\partial x}\right) + Q_+\left(\frac{\partial A}{\partial x}\frac{\partial \phi}{\partial y} - \frac{\partial A}{\partial y}\frac{\partial \phi}{\partial x} + \frac{\partial \phi}{\partial y}\right)}{P\left(\frac{\partial \phi}{\partial x}\right) + Q\left(\frac{\partial \phi}{\partial y}\right)} \\ &= \frac{Q(\xi(T^+), \eta(T^+))}{Q(\xi(T), \eta(T))} \\ &= \frac{\frac{ca_2((\xi_1 + \alpha) + \theta A)(1 - \beta)h_1}{b + A + \xi_1 + \alpha} - d_2(1 - \beta)h_1}{\frac{ca_2((\xi_1 + \alpha) + \theta A)h_1}{b + A + \xi_1} - d_2 h_1},\end{aligned}$$

$$\begin{aligned}\mu &= \Delta_1 \exp\Big[\int_0^T \Big(\frac{\partial P}{\partial x}(\xi(t),\eta(t)) + \frac{\partial Q}{\partial y}(\xi(t),\eta(t))\Big)\,\mathrm{d}t\Big]\\ &= \Delta_1 \exp\Big[\ln\frac{1}{1-\beta} + \ln\frac{\xi_1}{\xi_1+\alpha} - \int_0^T \Big(a_1\xi(t) - \frac{a_2\xi(t)\eta(t)}{(b+A+\xi(t))^2}\Big)\,\mathrm{d}t\Big]\\ &< \Delta_1\left(\frac{1}{1-\beta}\,\frac{\xi_1}{\xi_1+\alpha}\right)\\ &= \frac{\dfrac{ca_2((\xi_1+\alpha)+\theta A)h_1\xi_1}{b+A+\xi_1+\alpha} - d_2h_1\xi_1}{\dfrac{ca_2(\xi_1+\theta A)h_1(\xi_1+\alpha)}{b+A+\xi_1} - d_2h_1(\xi_1+\alpha)}.\end{aligned}$$

Let $H(x,y) = \frac{ca_2(x+\theta A)h_1y}{b+A+x} - d_2h_1y$; if $H(\xi_1+\alpha,\xi_1) < H(\xi_1,\xi_1+\alpha)$, $\mu < 1$, and hence, the unilateral order-1 periodic solution of system (3.1) is orbitally asymptotically stable.

3.2. Lower-threshold impulsive model

When predator populations are too small, take measures to increase y proportionally. Then, we get another unilateral state-feedback impulse control system:

$$\begin{cases}\left.\begin{aligned}\frac{dx}{dt} &= \frac{rx}{1+ky} - d_1x - a_1x^2 - \frac{a_2xy}{b+A+x},\\ \frac{dy}{dt} &= \frac{ca_2(x+\theta A)y}{b+A+x} - d_2y,\end{aligned}\right\} & y \neq h_2,\\ \left.\begin{aligned}\Delta x &= 0,\\ \Delta y &= \delta y,\end{aligned}\right\} & y = h_2.\end{cases} \tag{3.2}$$

The impulse set is

$$M_2 = \{(x,y) \mid x > 0, y = h_2\}.$$

The phase set is

$$N_2 = \{(x,y) \mid x > 0, y = (1+\delta)\,h_2\}.$$

Theorem 3.3. *System* (3.2) *possesses unilateral order-1 periodic solutions if* $y^* > h_2$.

Proof. As shown in Figure 2, we take a point $A_1(x_{A_1},(1+\delta)\,h_2)$ on N_2, $\forall\varepsilon > 0$, $x_{A_1} < \varepsilon$, the trajectory from A_1 intersects M_2 at M_A, and M_A maps to A_2 under impulsive action. We get

$$F(A_1) = x_{A_2} - x_{A_1} > 0.$$

We also take a point B_1 on N_2 such that $x_{B_1} > x_{E^*}$, the trajectory from B_1 intersects M_2 at M_B, and $x_{M_B} < x_{E^*}$. M_B maps to B_2 under impulsive action and $x_{B_2} = x_{M_B}$. So $x_{B_2} < x_{E^*} < x_{B_1}$. Then, we get

$$F(B_1) = x_{B_2} - x_{B_1} < 0.$$

By the continuity of the successor function [18], $\exists P \in (A_1,B_1)$ such that $F(P) = 0$. So, system (3.2) possesses unilateral order-1 periodic solutions.

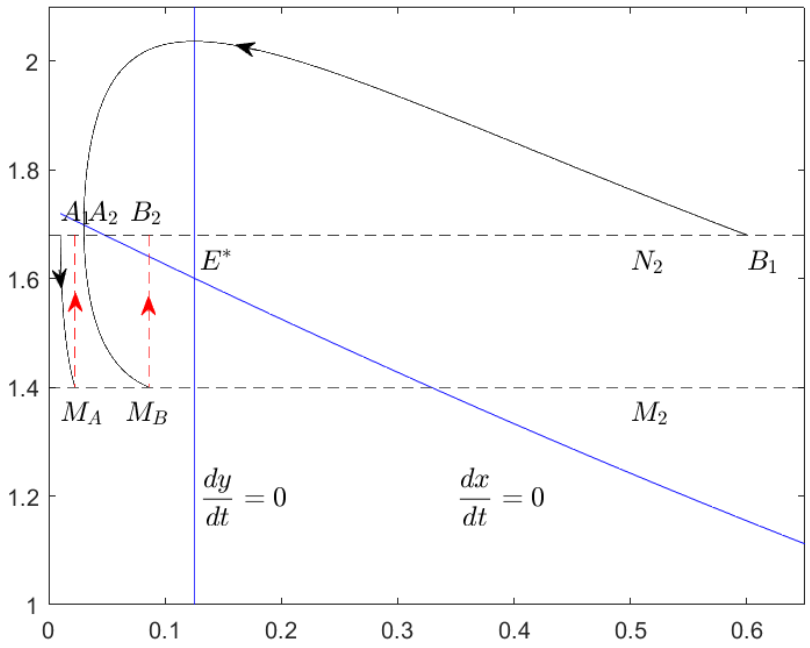

Figure 2. Unilateral order-1 periodic solutions.

Theorem 3.4. *The unilateral order-1 periodic solution of system* (3.2) *is orbitally asymptotically stable.*

Proof. Let $x = \xi(t)$, $y = \eta(t)$ be the unilateral order-1 periodic solution, and the period be T. As can be seen from system (3.2),

$$P(x,y) = \frac{rx}{1+ky} - d_1x - a_1x^2 - \frac{a_2xy}{b+A+x},$$

$$Q(x,y) = \frac{ca_2(x+\theta A)y}{b+A+x} - d_2y,$$

$$A(x,y) = 0, B(x,y) = \delta y, \phi(x,y) = y - h_2;$$

$$(\xi(0), \eta(0)) = (\xi_0, \eta_0),$$

$$(\xi(T), \eta(T)) = (\xi_1, \eta_1) = (\xi_1, h_2),$$

$$(\xi(T^+), \eta(T^+)) = (\xi_0, \eta_0) = (\xi_1, (1+\delta)h_2).$$

We get

$$\frac{\partial P}{\partial x} = \frac{r}{1+ky} - d_1 - 2a_1x - \frac{a_2y(b+A)}{(b+A+x)^2},$$

$$\frac{\partial Q}{\partial y} = \frac{ca_2(x+\theta A)}{b+A+x} - d_2,$$

$$\frac{\partial A}{\partial x}=0,\frac{\partial A}{\partial y}=0,\frac{\partial B}{\partial x}=0,\frac{\partial B}{\partial y}=\delta,\frac{\partial \phi}{\partial x}=0,\frac{\partial \phi}{\partial y}=1.$$

Then,

$$\begin{aligned}\Delta_1 &= \frac{P_+\left(\frac{\partial B}{\partial y}\frac{\partial \phi}{\partial x}-\frac{\partial B}{\partial x}\frac{\partial \phi}{\partial y}+\frac{\partial \phi}{\partial x}\right)+Q_+\left(\frac{\partial A}{\partial x}\frac{\partial \phi}{\partial y}-\frac{\partial A}{\partial y}\frac{\partial \phi}{\partial x}+\frac{\partial \phi}{\partial y}\right)}{P(\frac{\partial \phi}{\partial x})+Q(\frac{\partial \phi}{\partial y})}\\ &= \frac{Q(\xi(T^+),\eta(T^+))}{Q(\xi(T),\eta(T))}\\ &= \frac{\frac{ca_2(\xi_1+\theta A)(1+\delta)h_2}{b+A+\xi_1}-d_2(1+\delta)h_2}{\frac{ca_2(\xi_1+\theta A)h_2}{b+A+\xi_1}-d_2h_2}\\ &= 1+\delta,\end{aligned}$$

$$\begin{aligned}\mu &= \Delta_1\exp\left[\int_0^T\left(\frac{\partial P}{\partial x}(\xi(t),\eta(t))+\frac{\partial Q}{\partial y}(\xi(t),\eta(t))\right)\mathrm{d}t\right]\\ &= \Delta_1\exp\left[-\ln(1+\delta)-\int_0^T\left(a_1\xi(t)-\frac{a_2\xi(t)\eta(t)}{(b+A+\xi(t))^2}\right)\mathrm{d}t\right]\\ &< \Delta_1\frac{1}{1+\delta}\\ &= (1+\delta)\frac{1}{1+\delta}\\ &= 1.\end{aligned}$$

Hence, $\mu<1$, and the unilateral order-1 periodic solution of system (3.2) is orbitally asymptotically stable.

4. Bilateral state-feedback impulse controls

We get a bilateral state-feedback impulse control system:

$$\begin{cases}\left.\begin{aligned}\frac{dx}{dt}&=\frac{rx}{1+ky}-d_1x-a_1x^2-\frac{a_2xy}{b+A+x},\\ \frac{dy}{dt}&=\frac{ca_2(x+\theta A)y}{b+A+x}-d_2y,\end{aligned}\right\} x>\frac{3}{2}x^*,\ y\neq h_1,h_2,\\ \left.\begin{aligned}\Delta x_1&=\alpha,\\ \Delta y_1&=-\beta y,\end{aligned}\right\} 0<x<\frac{3}{2}x^*,\ y=h_1,\\ \left.\begin{aligned}\Delta x_2&=0,\\ \Delta y_2&=\delta y,\end{aligned}\right\} y=h_2.\end{cases}\tag{4.1}$$

Next, let's suppose that $\alpha < x^*$.

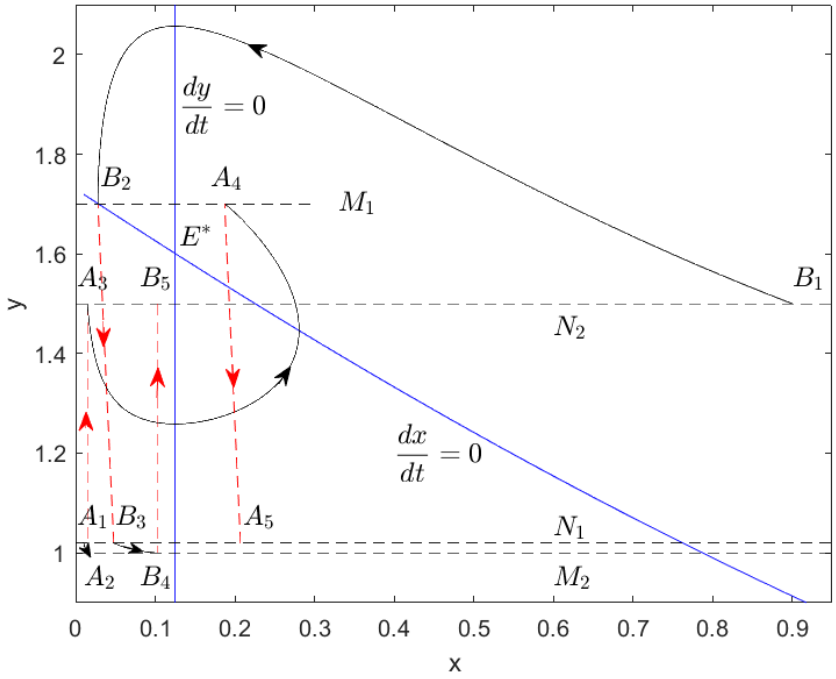

Figure 3. Bilateral order-1 periodic solutions.

Theorem 4.1. *System* (4.1) *possesses bilateral order-1 periodic solutions if* $h_1 > (1+\delta)\, h_2 > (1-\beta)\, h_1 > h_2$.

Proof. As shown in Figure 3, firstly, we take a point A_4 on M_1 such that $x_{A_4} > x_{E^*}$, so we can find a ponit A_3 on N_2 such that the trajectory from A_3 intersects M_1 at A_4 and $x_{A_3} < x_{E^*}$. We can also find a point A_2 on M_2 such that A_2 maps to A_3 under impulsive action and $x_{A_2} = x_{A_3}$. We can find a point A_1 on N_1 such that the trajectory from A_1 intersects M_2 at A_2 and $x_{A_1} < x_{A_2}$. So $x_{A_1} < x_{E^*}$. Additionally, A_4 maps to A_5 on N_1 under impulsive action and $x_{A_5} = x_{A_4} + \alpha > x_{E^*}$. So $x_{A_1} < x_{E^*} < x_{A_5}$. Then, we get

$$F(A_1) = x_{A_5} - x_{A_1} > 0.$$

At the same time, we take a point $B_2(x_{B_2}, h_1)$ on M_1. $\forall \varepsilon > 0$, when $x_{B_2} < \varepsilon$, we can find a point B_1 such that the trajectory from B_1 intersects M_1 at B_2 and $x_{B_1} > x_{E^*}$. Then, B_2 maps to B_3 on N_1 under impulsive action and $x_{B_3} = x_{B_2} + \alpha < x_{E^*}$. Also, the trajectory from B_3 intersects M_2 at B_4 and $x_{B_4} < x_{E^*}$. Finally, B_4 maps to B_5 on N_2 under impulsive action and $x_{B_5} = x_{B_4}$. So $x_{B_5} < x_{E^*} < x_{B_1}$. Then, we get

$$F(B_1) = x_{B_5} - x_{B_1} < 0.$$

By the continuity of the successor function [18], $\exists P$ such that $F(P) = 0$. So system (4.1) possesses unilateral order-1 periodic solutions.

Theorem 4.2. *The bilateral order-1 periodic solution of system* (4.1) *is orbitally asymptotically stable if* $H(\xi_0, (1+\delta)(\xi_0-\alpha)) < H(\xi_0-\alpha, \xi_0)$.

Proof. Let $x = \xi(t)$, $y = \eta(t)$ be the unilateral order-1 periodic solution, and the period be T. As can be seen from system (4.1),

$$P(x,y) = \frac{rx}{1+ky} - d_1 x - a_1 x^2 - \frac{a_2 xy}{b+A+x},$$

$$Q(x,y) = \frac{ca_2(x+\theta A)y}{b+A+x} - d_2 y,$$

$$A_1(x,y) = 0, B_1(x,y) = \delta y, \phi_1(x,y) = y - h_2,$$

$$A_2(x,y) = \alpha, B_2(x,y) = -\beta y, \phi_2(x,y) = y - h_1;$$

$$(\xi(0), \eta(0)) = (\xi_0, \eta_0),$$

$$(\xi(T_1), \eta(T_1)) = (\xi_1, \eta_1) = (\xi_1, h_2),$$

$$(\xi(T_1^+), \eta(T_1^+)) = (\xi_1, (1+\delta)h_2),$$

$$(\xi(T_1^+ + T_2), \eta(T_1^+ + T_2)) = (\xi_2, \eta_2) = (\xi_0 - \alpha, h_1),$$

$$(\xi(T_1^+ + T_2^+), \eta(T_1^+ + T_2^+)) = (\xi_0, \eta_0) = (\xi_0, (1-\beta)h_1).$$

We get

$$\frac{\partial P}{\partial x} = \frac{r}{1+ky} - d_1 - 2a_1 x - \frac{a_2 y(b+A)}{(b+A+x)^2},$$

$$\frac{\partial Q}{\partial y} = \frac{ca_2(x+\theta A)}{b+A+x} - d_2,$$

$$\frac{\partial A_1}{\partial x} = 0, \frac{\partial A_1}{\partial y} = 0, \frac{\partial B_1}{\partial x} = 0, \frac{\partial B_1}{\partial y} = \delta, \frac{\partial \phi_1}{\partial x} = 0, \frac{\partial \phi_1}{\partial y} = 1,$$

$$\frac{\partial A_2}{\partial x} = 0, \frac{\partial A_2}{\partial y} = 0, \frac{\partial B_2}{\partial x} = 0, \frac{\partial B_2}{\partial y} = -\beta, \frac{\partial \phi_2}{\partial x} = 0, \frac{\partial \phi_2}{\partial y} = 1.$$

Then,

$$\begin{aligned}\Delta_1 &= \frac{Q\left(\xi\left(T_1^+\right), \eta\left(T_1^+\right)\right)}{Q(\xi(T_1), \eta(T_1))} \\ &= \frac{\frac{ca_2(\xi_1+\theta A)(1+\delta)h_2}{b+A+\xi_1} - d_2(1+\delta)h_2}{\frac{ca_2(\xi_1+\theta A)h_2}{b+A+\xi_1} - d_2 h_2} \\ &= 1+\delta,\end{aligned}$$

$$\Delta_2 = \frac{Q\left(\xi\left(T_1^+ + T_2^+\right), \eta\left(T_1^+ + T_2^+\right)\right)}{Q\left(\xi\left(T_1^+ + T_2\right), \eta\left(T_1^+ + T_2\right)\right)}$$

$$= \frac{\frac{ca_2(\xi_0+\theta A)(1-\beta)h_1}{b+A+\xi_0} - d_2(1-\beta)h_1}{\frac{ca_2(\xi_0-\alpha+\theta A)h_1}{b+A+\xi_0-\alpha} - d_2h_1},$$

$$\begin{aligned}
\mu_2 &= \Delta_1\Delta_2 \exp\Big[\int_0^{T_1+T_2}\Big(\frac{\partial P}{\partial x}(\xi(t),\eta(t)) + \frac{\partial Q}{\partial y}(\xi(t),\eta(t))\Big)\,\mathrm{d}t\Big] \\
&= \Delta_1\Delta_2 \exp\Big[\ln\frac{1}{1-\beta} + \ln\frac{\xi_0-\alpha}{\xi_0} - \int_0^{T_1+T_2}\Big(a_1\xi(t) - \frac{a_2\xi(t)\eta(t)}{(b+A+\xi(t))^2}\Big)\,\mathrm{d}t\Big] \\
&< (1+\delta)\frac{\frac{ca_2(\xi_0+\theta A)h_1(1-\beta)}{b+A+\xi_0} - d_2h_1(1-\beta)}{\frac{ca_2(\xi_0-\alpha+\theta A)h_1}{b+A+\xi_0-\alpha} - d_2h_1}\frac{1}{1-\beta}\frac{\xi_0-\alpha}{\xi_0} \\
&= \frac{\frac{ca_2(\xi_0+\theta A)h_1(1+\delta)(\xi_0-\alpha)}{b+A+\xi_0} - d_2h_1(1+\delta)(\xi_0-\alpha)}{\frac{ca_2(\xi_0-\alpha+\theta A)h_1\xi_0}{b+A+\xi_0-\alpha} - d_2h_1\xi_0}.
\end{aligned}$$

If $H(\xi_0, (1+\delta)(\xi_0-\alpha)) < H(\xi_0-\alpha, \xi_0)$ with $\mu < 1$, then the bilateral order-1 periodic solution of system (4.1) is orbitally asymptotically stable.

5. Numerical simulation

First, we perform numerical simulations on system (2.1). We fix the parameters as follows:

$$r = 2; k = 1; a_1 = 0.6; a_2 = 2; b = 5;$$
$$d_1 = 0.3; d_2 = 0.4; c = 1; \theta = 0.5; A = 3.$$

Figure 4 shows the stability of E^* under these parameters, i.e., E^* is stable, which verifies the theoretical results.

Then, we change the values of parameters A and k separately. As can be seen from Figures 4–6, as parameter A decreases, x gradually increases and y gradually decreases. This suggests that additional food has a negative effect on prey populations and a positive effect on predator populations. And as can be seen from the Figures 4 and 7, the existence of parameter k has a negative effect on predator populations, but no effect on prey populations.

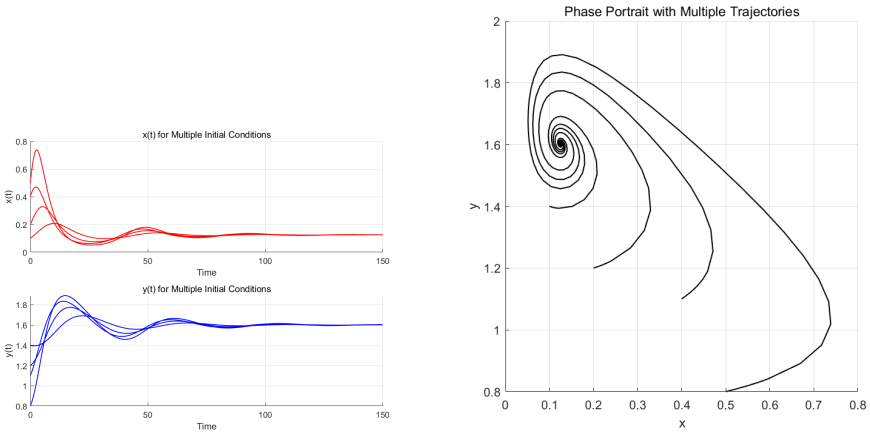

(a) $x(t)$, $y(t)$ for Multiple Initial Conditions. (b) Phase Portrait with Multiple Trajectories.

Figure 4. E^* is globally asymptotically stable, $k = 1$, and $A = 3$.

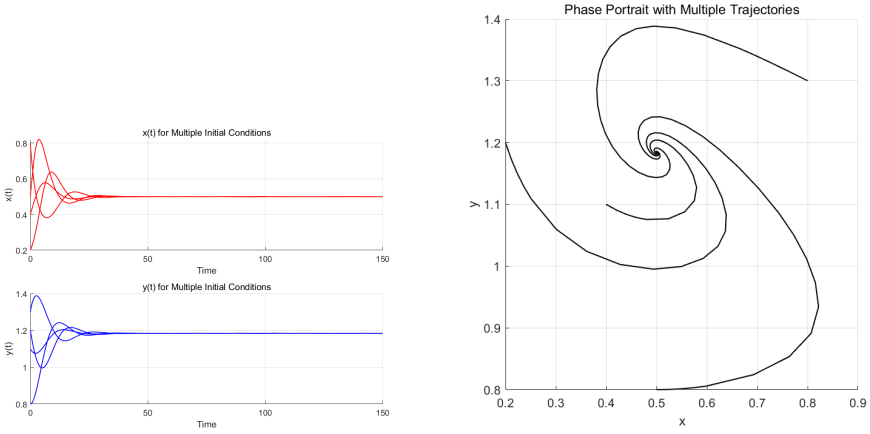

(a) $x(t)$, $y(t)$ for Multiple Initial Conditions. (b) Phase Portrait with Multiple Trajectories.

Figure 5. E^* is globally asymptotically stable, $k = 1$, and $A = 2$.

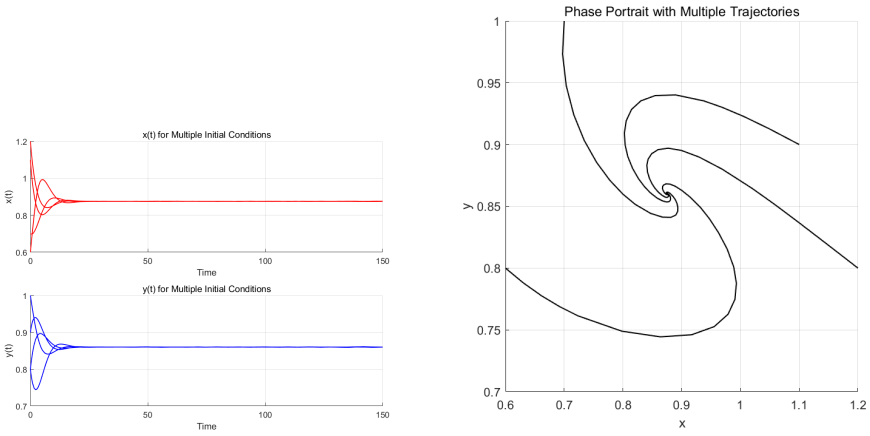

(a) $x(t)$, $y(t)$ for Multiple Initial Conditions. (b) Phase Portrait with Multiple Trajectories.

Figure 6. E^* is globally asymptotically stable, $k = 1$, and $A = 1$.

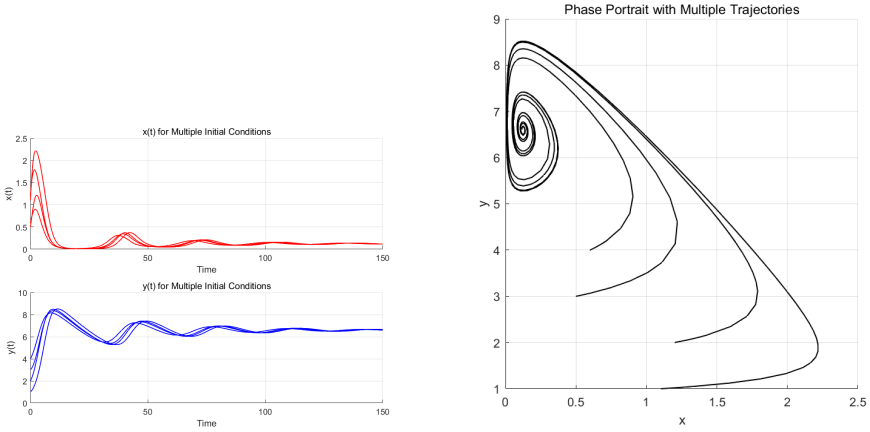

(a) $x(t)$, $y(t)$ for Multiple Initial Conditions. (b) Phase Portrait with Multiple Trajectories.

Figure 7. E^* is globally asymptotically stable, $k = 0$, and $A = 3$.

Next, we perform numerical simulations on system (3.1). Set the impulse parameter values as follows:

$$h_1 = 1.5; \beta = 0.3; \alpha = 0.12.$$

Figure 8 shows that x and y have periodic trends, and there are periodic orbits near the positive equilibrium point.

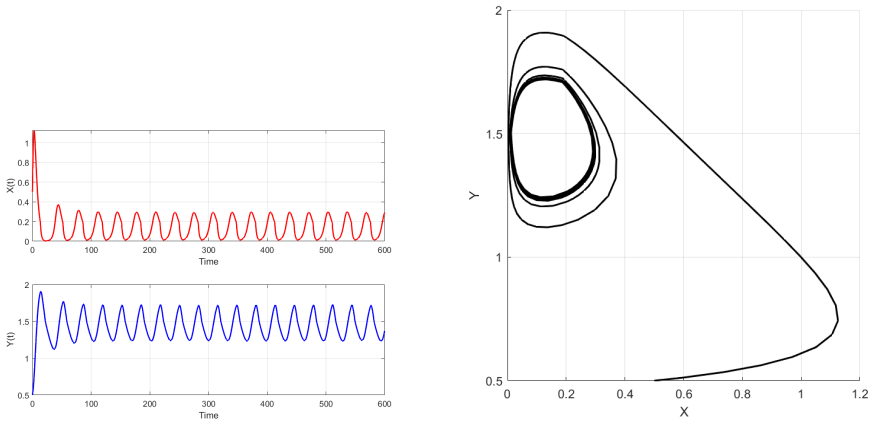

(a) Time series graph of $x(t)$ and $y(t)$. (b) Phase Portrait.

Figure 8. System (3.1) possesses unilateral order-1 periodic solutions. $h_1 = 1.5$; $\beta = 0.3$; $\alpha = 0.12$.

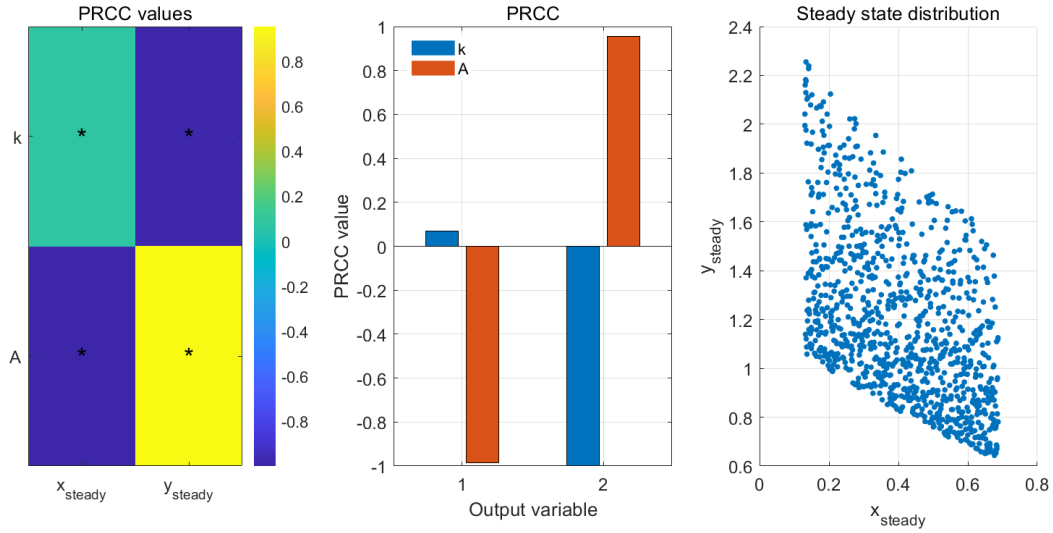

Figure 9. Partial rank correlation coefficient sensitivity analysis.

Finally, we perform a sensitivity analysis on parameters k and A to assess the degree of influence of the parameters on the model output results. Figure 9 shows the analysis results. The results indicate that both parameters have a significant impact on system (2.1)'s stable positive equilibrium point. Specifically, parameter k has a negligible effect on the prey population but exhibits a strong negative correlation with the predator population (partial rank correlation coefficient (PRCC) value is negative, and $p < 0.05$), indicating that as fear increases, the predator population decreases. Parameter A exhibits a strong negative correlation with the prey population (PRCC value is negative, and $p < 0.05$),

whereas parameter A shows a significant positive correlation with the predator population (PRCC value is positive, $p < 0.05$), indicating that additional food helps to improve the survival and growth of predators but is not conducive to the growth of prey. Also, the stable positive equilibrium point of the system converges to a relatively stable range in most samples, and the scatter plot shows that the system has a certain degree of robustness to parameter changes.

6. Discussion

At present, traditional grassland rodent pest control methods primarily rely on chemical rodenticides or manual culling. While these approaches can temporarily suppress vole populations in the short term, they inevitably cause soil and water pollution, damage biodiversity, and fail to fundamentally balance the predator-prey relationship, ultimately leading to recurrent rodent outbreaks. Against this backdrop, developing a predator-prey system model that integrates ecological regulation and precision intervention has become an urgent need for grassland ecological conservation and sustainable management. Such a model enables the quantitative analysis of the mechanisms underlying key ecological factors, including prey refuges, fear effects, and additional food , and, when combined with state-feedback impulse control strategies, facilitates dynamic, targeted regulation of the vole-weasel population system. This study directly responds to this critical demand, offering a theoretically rigorous and practically feasible alternative to conventional control methods that addresses the limitations of traditional approaches while advancing the sustainable management of grassland ecosystems.

The theoretical model constructed in this study is deeply rooted in the ecological dynamics of grassland predator-prey systems, with the state-feedback impulse control mechanism serving as a critical bridge between abstract mathematical theory and practical ecological management. By integrating this control framework into the basic predator-prey model, we achieved dynamic, targeted regulation of the vole-weasel system, which not only advances the theoretical development of impulsive differential equations in population ecology but also provides an actionable technical paradigm for emergency intervention in grassland ecosystems, with profound ecological management significance.

From a theoretical perspective, the unilateral and bilateral state-feedback impulse control systems established in this study rigorously prove the existence of order-1 periodic solutions under specific parameter conditions and derive the sufficient conditions for orbit asymptotic stability. These theoretical results confirm that the proposed control strategy can drive the system to converge to a stable periodic state, ensuring the long-term sustainability of the predator-prey population structure.

In terms of ecological practice, the differentiated impulse intervention strategy proposed in this study directly addresses the extreme population crises commonly faced by grassland ecosystems, with clear ecological logic and practical value. When the weasel (predator) population reaches the preset upper threshold h_1 and the vole (prey) density is low ($0 < x < \frac{3}{2}x^*$), the combined intervention of supplementing vole populations and removing a portion of weasels achieves a dual ecological goal: On the one hand, it alleviates the excessive predation pressure of weasels on voles, preventing vole extinction and the subsequent collapse of the grassland food chain; on the other hand, it avoids large-scale migration of weasels caused by food shortages, which would otherwise disrupt the regional ecological balance. When the weasel population drops below the lower threshold h_2, the targeted introduction of weasels effectively prevents the risk of predator extinction, which in turn curbs the outbreak of field mice (voles) due to the loss of natural predators. This intervention directly mitigates

severe ecological problems such as grassland degradation and desertification caused by overgrazing of voles, protecting the structural stability and functional integrity of the grassland ecosystem.

Notably, the bilateral control mechanism proposed in this study represents a significant improvement over unilateral control strategies. This mechanism realizes proactive, coordinated management of both predator and prey populations. By dynamically adjusting the population sizes of voles and weasels based on real-time ecological thresholds, it significantly enhances the resilience and recovery capacity of the grassland ecosystem, enabling the system to quickly return to a stable state after disturbances. This mechanism is particularly suitable for the restoration of grassland ecosystems disturbed by human activities (e.g., overgrazing, habitat destruction, and invasive species), providing a scientifically rigorous and practically feasible solution for formulating emergency ecological intervention measures.

Moving forward, subsequent research can further develop the model by integrating more nuanced ecological processes, including seasonal environmental variability, multi-species interspecific interactions, and the demographic impacts of climate change, to strengthen its ecological realism and adaptability to heterogeneous real-world grassland ecosystems. In addition, long-term field-based monitoring and rigorous empirical validation of the proposed state-feedback impulse control strategy in natural grassland systems will be indispensable to calibrate intervention parameters, assess long-term ecological outcomes, and translate this theoretical framework into scalable, practical solutions for sustainable grassland ecosystem management.

7. Conclusions

In this study, we develop a predator-prey model incorporating the effects of fear and additional food provision. We analyze the existence and stability of equilibrium points and demonstrate that, under certain conditions, the positive equilibrium is globally asymptotically stable. Furthermore, building upon this baseline model, we introduce both unilateral and bilateral impulsive control strategies and investigate the existence and stability of order-1 periodic solutions.

Our findings indicate that the provision of additional food exerts a negative influence on the prey population while benefiting the predator population. In contrast, the effect of fear is relatively minor on the prey but shows a strong negative correlation with the predator population. Thus, both fear and additional food are identified as key factors influencing the stability of predator-prey dynamics. Appropriate regulation of these parameters can facilitate the achievement of ecosystem stability and management objectives.

Moreover, a unilateral state-dependent impulsive control strategy is proposed, triggered when the predator population reaches a predefined threshold while the prey density remains low. This intervention involves the artificial replenishment of prey and the simultaneous removal of a proportion of predators. Such a measure simulates emergency management actions—such as prey restocking, protective measures, or predator culling—aimed at mitigating excessive predation pressure and preventing prey extinction. This mechanism highlights the resilience and recovery potential of ecosystems under active management and offers insights for targeted species conservation.

In addition, a bilateral impulsive control strategy extends the unilateral approach by incorporating active management of the predator population. When predator density falls below a lower threshold, a second type of impulse is activated, involving the introduction of predators to prevent functional loss due to low population levels. This strategy is essential for maintaining the ecological role of predators

and contributes to more holistic ecosystem regulation. The bilateral control framework embodies a "bidirectional restoration" philosophy, dynamically managing both predator and prey populations to preserve ecosystem integrity and functionality.

Several directions for future research remain. First, the current model does not incorporate time delays or spatial heterogeneity, which are common in real ecosystems. Future work could integrate delayed responses in growth or predation terms to better reflect memory or physiological lags. Second, regarding impulsive control, the present framework assumes impulses of fixed magnitude triggered by threshold conditions. Subsequent studies could explore optimal control strategies to determine more efficient timing and intensity of interventions, or develop stochastic impulsive models to account for environmental variability.

Use of AI tools declaration

The authors declare they have not used Artificial Intelligence (AI) tools in the creation of this article.

Acknowledgments

This work is supported by NSFC (No.11701026).

Conflict of interest

The authors declare there are no conflicts of interest.

References

1. S. Creel, D. Christianson, Relationships between direct predation and risk effects, *Trends Ecol. Evol.*, **23** (2008), 194–201. https://doi.org/10.1016/j.tree.2007.12.004
2. E. L. Preisser, D. I. Bolnick, The many faces of fear: comparing the pathways and impacts of nonconsumptive predator effects on prey populations, *PLoS One*, **3** (2008), e2465. https://doi.org/10.1371/journal.pone.0002465
3. X. Zhao, L. Yu, X. Li, Dynamics analysis of a predator-prey model incorporating fear effect in prey species, *AIMS Math.*, **10** (2025), 12464–12492. https://doi.org/10.3934/math.2025563
4. S. L. Lima, Nonlethal effects in the ecology of predator-prey interactions: What are the ecological effects of anti-predator decision-making? *Bioscience*, **48** (1998), 25–34. https://doi.org/10.2307/1313225
5. L. Y. Zanette, A. F. White, M. C. Allen, M. Clinchy, Perceived predation risk reduces the number of offspring songbirds produce per year, *Science*, **334** (2011), 1398–1401. https://doi.org/10.1126/science.1210908
6. S. K. Sasmal, Population dynamics with multiple Allee effects induced by fear factors–A mathematical study on prey-predator interactions, *Appl. Math. Modell.*, **64** (2018), 1–14. https://doi.org/10.1016/j.apm.2018.07.021

7. S. Mondal, A. Maiti, G. P. Samanta, Effects of fear and additional food in a delayed predator-prey model, *Biophys. Rev. Lett.*, **13** (2018), 157–177. https://doi.org/10.1142/S1793048018500091
8. S. Sharma, G. P. Samanta, Dynamical behaviour of age-selective harvesting of a prey-predator system, *Int. J. Dyn. Control*, **6** (2018), 550–560. https://doi.org/10.1007/s40435-017-0337-3
9. D. Pal, G. S. Mahapatra, G. P. Samanta, Optimal harvesting of prey-predator system with interval biological parameters: A bioeconomic model, *Math. Biosci.*, **241** (2013), 181–187. https://doi.org/10.1016/j.mbs.2012.11.007
10. M. R. Wade, M. P. Zalucki, S. D. Wratten, K. A. Robinson, Conservation biological control of arthropods using artificial food sprays: Current status and future challenges, *Biol. Control*, **45** (2008), 185–199. https://doi.org/10.1016/j.biocontrol.2007.10.024
11. P. D. Srinivasu, B. S. Prasad, M. Venkatesulu, Biological control through provision of additional food to predators: a theoretical study, *Theor. Popul Biol.*, **72** (2007), 111–120. https://doi.org/10.1016/j.tpb.2007.03.011
12. S. Ghorai, S. Poria, Impacts of additional food on diffusion induced instabilities in a predator-prey system with mutually interfering predator, *Chaos, Solitons Fractals*, **103** (2017), 68–78. https://doi.org/10.1016/j.chaos.2017.05.031
13. T. Wang, L. Chen, Nonlinear analysis of a microbial pesticide model with impulsive state feedback control, *Nonlinear Dyn.*, **65** (2011), 1–10. https://doi.org/10.1007/s11071-010-9828-x
14. S. Tang, B. Tang, A. Wang, Y. Xiao, Holling II predator-prey impulsive semi-dynamic model with complex Poincaré map, *Nonlinear Dyn.*, **81** (2015), 1575–1596. https://doi.org/10.1007/s11071-015-2092-3
15. P. S. Simeonov, D. D. Bainov, Orbital stability of the periodic solutions of autonomous systems with impulse effect, *Int. J. Syst. Sci.*, **19** (1988), 2561–2585. https://doi.org/10.1080/00207728808547133
16. G. Birkhoff, G. C. Rota, *Ordinary Differential Equations*, Ginn and Company, Boston, 1962.
17. L. Perko, *Differential Equations and Dynamical Systems*, Springer, New York, 2001. https://doi.org/10.1007/978-1-4613-0003-8
18. G. Pang, L. Chen, Periodic solution of the system with impulsive state feedback control, *Nonlinear Dyn.*, **78** (2014), 743–753. https://doi.org/10.1007/s11071-014-1473-3
19. Y. Tian, J. Zhu, J. Zheng, K. Sun, Modeling and analysis of a prey-predator system with prey habitat selection in an environment subject to stochastic disturbances, *Electron. Res. Arch.*, **33** (2025), 744–767. https://doi.org/10.3934/era.2025034
20. X. Meng, L. Chen, Periodic solution and almost periodic solution for a nonautonomous Lotka–Volterra dispersal system with infinite delay, *J. Math. Anal. Appl.*, **339** (2008), 125–145. https://doi.org/10.1016/j.jmaa.2007.05.084
21. S. Gao, S. Yuan, Dynamics of a tri-trophic level model with excess food nutrient content and intraguild predation structure, *J. Biol. Syst.*, **32** (2024), 1133–1168. https://doi.org/10.1142/S0218339024500384
22. X. Duan, S. Yuan, M. Martcheva, Habitat adaption promotes the evolution of predator species, *Z. Angew. Math. Phys.*, **74** (2023), 10. https://doi.org/10.1007/s00033-022-01904-8

23. P. Wu, S. Zhang, X. Wang, H. Wang, Spatiotemporal cholera dynamics with antibiotic resistance and vaccination via demographic-epidemic data in Zimbabwe, *J. Math. Biol.*, **92** (2026), 42. https://doi.org/10.1007/s00285-026-02360-y

24. P. Wu, C. Fang, Spatiotemporal dynamics of syphilis in Xinjiang via a demographic geographic data-validated reaction diffusion model, *J. Math. Phys.*, **66** (2025), 062704. https://doi.org/10.1063/5.0273893

25. Y. Cai, W. Wang, Dynamics of a parasite-host epidemiological model in spatial heterogeneous environment, *Discrete Contin. Dyn. Syst. - Ser. B*, **20** (2015), 989–1013. https://doi.org/10.3934/dcdsb.2015.20.989

26. X. Xie, H. Yu, J. Fang, Z. Cao, Q. Wang, M. Zhao, Dynamics analysis of autonomous and nonautonomous predator-prey models with nonlinear harvesting, *Electron. Res. Arch.*, **33** (2025), 6096–6140. https://doi.org/10.3934/era.2025271

27. O. Nave, Y. Baron, M. Sharma, A semi-analytical method for solving problems on the role of prey taxis in a biological control-mathematical model, *J. Multiscale Modell.*, **10** (2019), 1850009. https://doi.org/10.1142/s1756973718500099

AIMS Press